Supporting Information

Vertically oriented arrays of polyaniline nanorods and their super electrochemical properties

Biplab K Kuila*, Bhanu Nandan, Marcus Böhme, Andreas Janke and Manfred Stamm#

Leibniz Institute of Polymer Research Dresden, Hohe Str. 6, D-01069 Dresden, Germany

S1. Experimental:

The AFM imaging was performed on as prepared samples on ITO substrate by a Dimensions 3100 (NanoScope IV – Controller) scanning force microscope in the tapping mode. The tip characteristics are as follows: spring constant 1.5-3.7 Nm^{-1}, resonant frequency 45/65 Hz, tip radius about 10 nm.

For SEM investigation, we transferred the block copolymer thin film before and after electro polymerization from rough ITO substrate to smooth cleaned silicon wafer. The silicon wafers [100] were cleaned successively in an ultrasonic bath (dichloromethane) for 15 minute and a 'piranha' bath (30% H_2O_2, 30% of NH_4OH, chemical Hazards) for 90 min at 75^0C, and then thoroughly rinsed with Millipore water and dried under Argon flow. Due to higher roughness of the ITO surface and as well as the very low thickness of the block copolymer thin film (30 nm), SEM images of the thin films on ITO did not revealed the template surface features, because electron beam passes the thin film and the image was a replica of the ITO substrate surface. After transferring the electro polymerized block copolymer thin film to silicon wafer, we removed the block copolymer by dissolving in chloroform to investigate the morphology of the polyaniline

---

for correspondence, email: #stamm@ipfdd.de and * Kuila@ipfdd.de

nanorods. The film was transferred from the ITO substrate by etching ITO coating by using Zinc and Hydrochloric acid and subsequently floating the thin film in to that solution. The film was then transferred to water and finally to silicon substrate using loop. SEM images were obtained with field emission electron microscopy (Zeiss Ultra 55 Gemini with FIB) operating at 3 kV.

Asylum Research (MFP-3D) is used to characterize electrical property of conducting polymer nanorods by Current sensing AFM (CS-AFM). Platinum-iridium (PtIr) coated cantilevers (spring constant 0.16-0.20 N/m, purchased from Nanosensors) were used to image the surface while the current was measured between the tip and the substrate at a given bias voltage. The contact can be made reliably and reproducibly between the tip and the substrate by applying a load force at 7-10 nN.

For TEM study, we first transferred the electpolymerized thin film on carbon coated grid and then remove the block copolymer template by dissolving in chloroform. TEM images were taken using transmission electron microscope(Libra 200) operating at 200 kV.

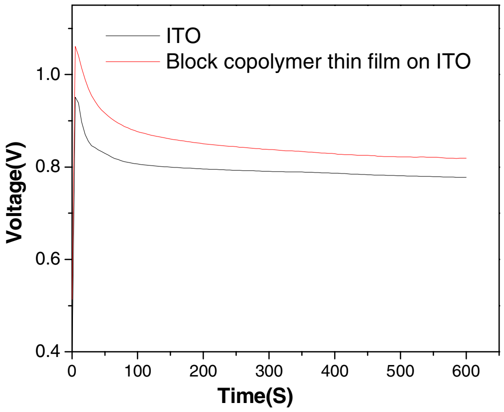

Figure S1. Time vs. voltage (V) plot of electropolymerization of aniline.

S2. AFM study:

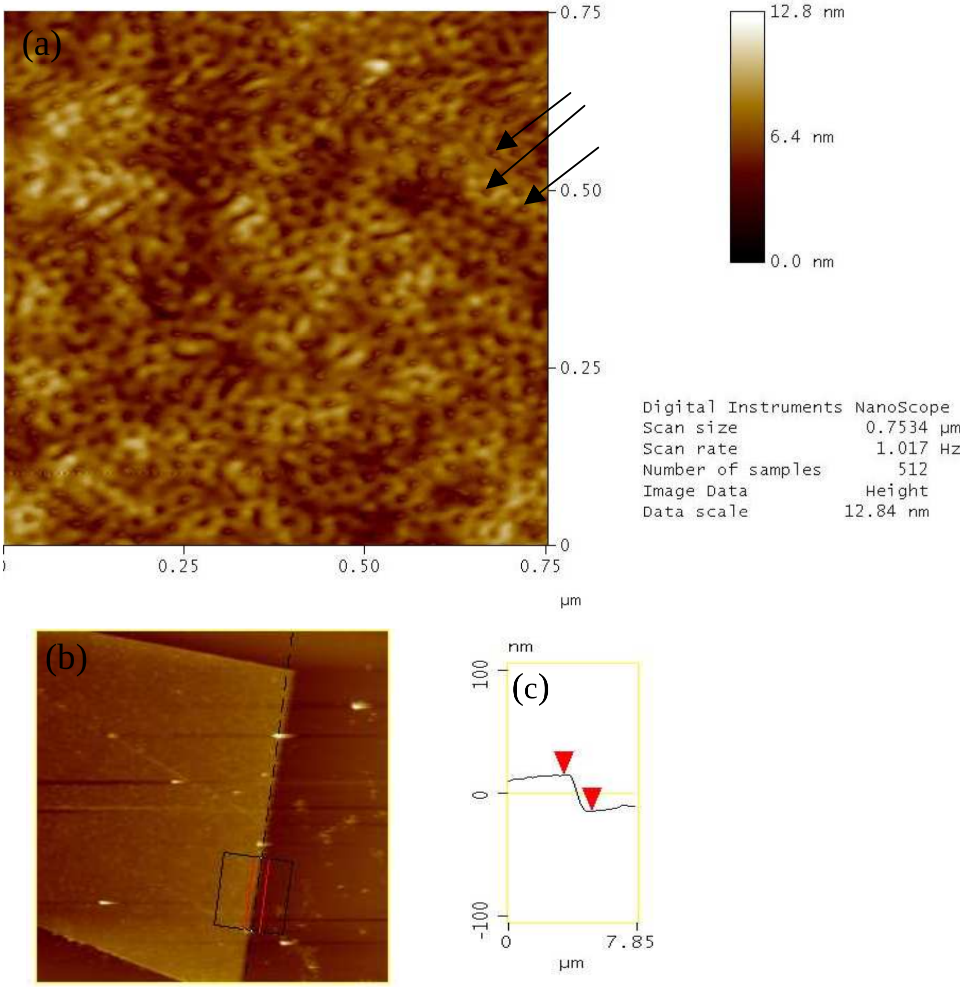

Figure S2 AFM height images of (a) block copolymer nanotemplate after electropolymerization. (b) AFM height images of this nanotemplate at low magnification. The total scale bar is 20 µm (c) corresponding height profile of the thin film across the edge of the film.

The large scale surface morphology (Figure S2a) of the thin film after electropolymerization remains intact. A careful observation of the AFM image in Figure S2a reveals that the polymerization only occurs inside the pores creating very small dots on the top (showing by arrow in the Figure S2a) of the hole which indicate that the polymerization just fills the holes with out random polymerization out side the template.

The thickness of the thin film after electropolymerization measured from the surface profile (Figure S2b and Figure S2c) is around 30 nm.

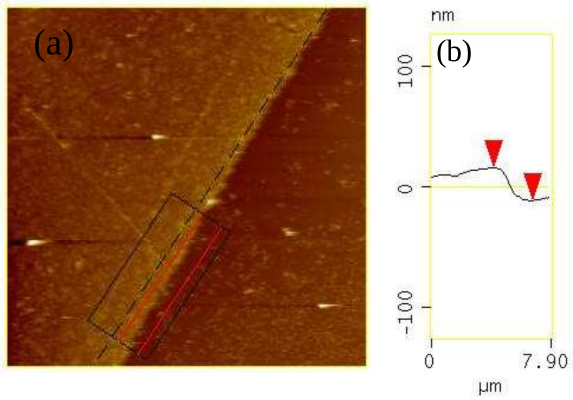

Figure S3 AFM height images of the thin film containing only arrays of polyaniline nanorods at low magnification. The total scale bar is 20 µm (b) corresponding height profile of the thin film across the edge of the film.

The average height of the nanorods has been calculated from the thickness of the thin film containing only polyaniline nanorods (after dissolving the electropolymerized nanotemplate in chloroform) and the average height of the nanorods is around 27 nm (Figure S3a and Figure S3b).

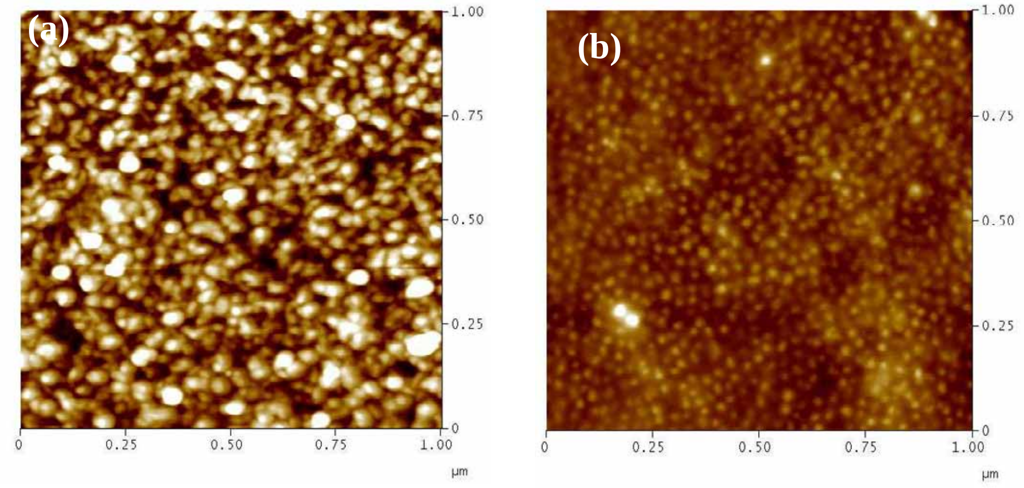

Figure S4 AFM height images of the thin film containing polyaniline deposited on bare ITO (b) polyaniline nanorods. The total scale bar is 1 µm.

The top surface of the polyaniline thin film on bare ITO [Figure S4(a)] looks like a thin film consisting of random PANI nanoparticle of different dimension and attached with each other. The film is also continuous with out any regular spacing between two polyaniline nanoparticle. Whereas in case of polyaniline deposited on ITO using block copolymer template [Figure S4b] consist of arrays polyaniline nanorods with 10 nm diameter with regular spacing. Form the two images it can be easily concluded that the mass deposited on bare ITO is higher than the PANI on block copolymer thin film.

S3. SEM study:

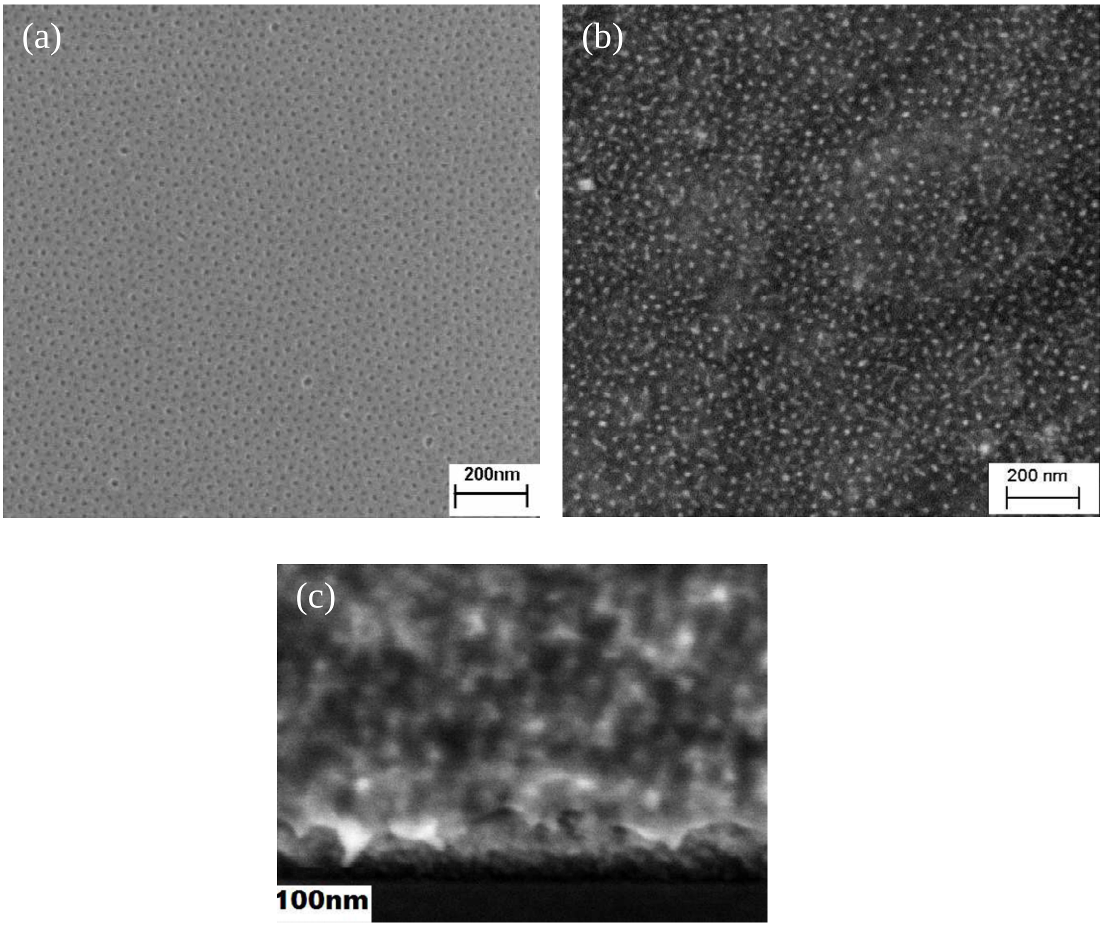

Figure S5. (a) SEM images of block copolymer nanotemplate deposited from 1,4 dioxane with a thickness about 30 nm and washed with methanol (b) Arrays of polyaniline nanorods after removing the template (c) cross sectional image of the thin film of polyaniline nanorods

The field emission scanning electron microscope image (Figure S5a) of the top portion of the nanoporous block copolymer template showed the cylindrical pores normal to the substrate throughout the entire surface of the film. After removing the template by dissolving in chloroform the Fe-SEM image showed highly dense arrays of polyaniline nanorods (Figure S5b) with average diameter ~10nm. The order and density of the nanorods are not very perfect, however the large scale morphology of the nanorods closely mirror that of the template.

S4. Current sensing AFM (CS-AFM) study of the polyaniline nanorods:

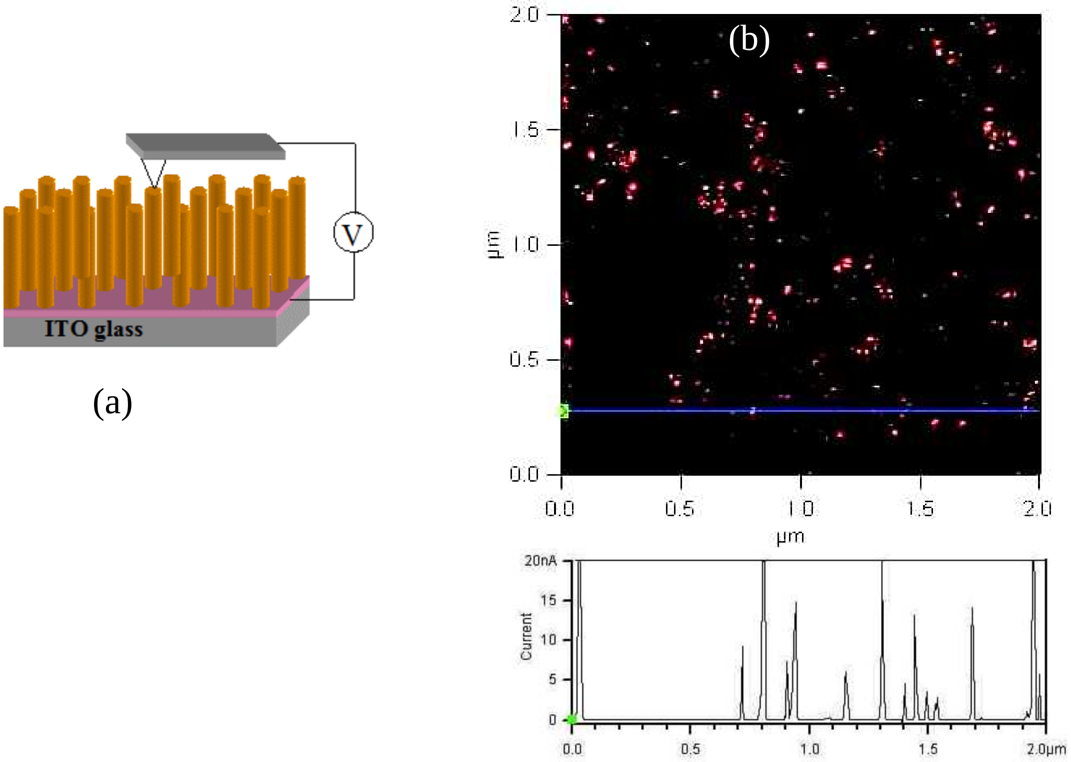

(a)

(c)

Figure-S6. Current sensing AFM images of polyaniline nanodots. (a) Schematic diagram for Current sensing AFM of PANI nanorods (b) Current image and (c) current profile.

A schematic diagram of measuring CSAFM is shown in the figure S6a, along with current sensing image (Figure S6b) at a bias voltage of 2 volt and current profile (Figure S6c). The I-V curves of PANI nanorods represent a characteristics curve for individual nanorods since the contacting diameter of CSAFM probe employed in this study was around 10 nm. The PANI nanorods appeared as bright spot in SPM image which is consistent with those in the current image. The current flowing through the individual nanorods is shown in the current profile plot (Figure S6c). The height of the different peaks correspond to the current passing through different nanorods. The current passing through different nanorods is not same which could be attributed to the nonuniform height of the nanorods as discussed earlier.

S5. Fourier transform infrared spectroscopy (FTIR) study:

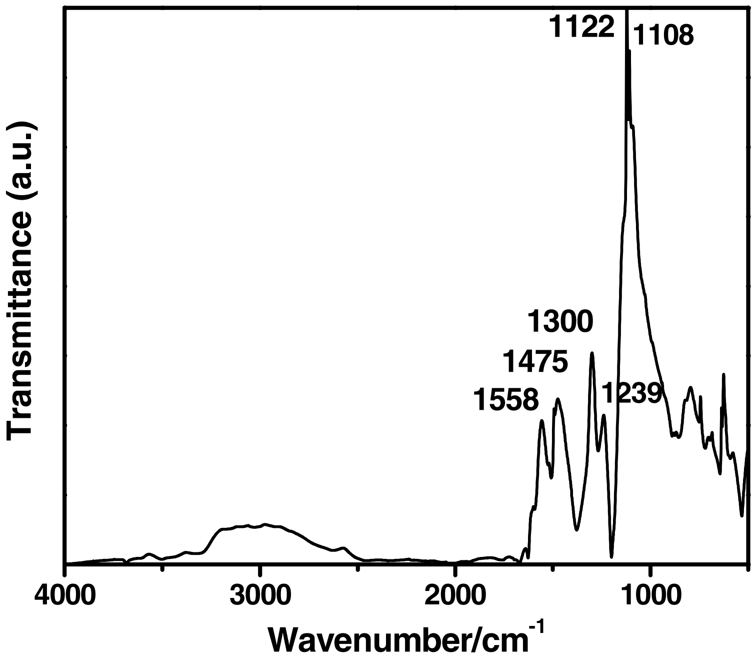

Figure S7. IR Spectra of electropolymerized polyaniline

In order to verify the polyaniline structure formed by electropolymerization, we perform the Fourier transform infrared spectroscopy (FTIR). The FTIR spectra of the polyaniline deposited on ITO using block copolymer nanotemplate is depicted in Figure S7. The characteristic peaks at 1558 cm^{-1} and 1475 cm^{-1} corresponds to quinoid ring and benzene ring respectively[S1, S2, S3]. The bands in the range of 1200-1400 cm^{-1} (1300 cm^{-1} and 1239 cm^{-1}) are the C-N stretching band of aromatic amine. The characteristic band of polyaniline base is the N=Q=N stretching band at 1122cm^{-1}. The bands at 1108 cm^{-1} can be ascribed to Cl-O stretching frequency of the perchlorate[S4] ion. From the FTIR study, it can be concluded that the electro polymerized PANI has both quinoid and benzene ring. Hence, the polyaniline is in the form of emeralidine salt where the corresponding anion is perchlorate ion. The formation of emeralidine salt by electropolymerization using constant current is also supported by previously reported work in the literature[S5].

S6. Calculation of electrodeposited mass of polyaniline:

The amount of polyaniline deposited per cm^2 using block copolymer thin film can be calculated from the real active area of the ITO exposed to the solution. For block copolymer thin film, the ITO surface is exposed to the solution only through cylindrical pores of around 8 nm diameter and polyaniline will be deposited only inside these cylindrical pores. Hence, by calculating the number of cylindrical pore in a particular area, we can calculate the total area of ITO exposed to solution. It is around 1.2×10^{11} for 1cm^2 for block copolymer thin film deposited on ITO. Assuming one aniline monomer deposited per 2.5 electron (considering emerlidine salt of polyaniline deposited by electropolymerization, see FTIR study), the amount of polyaniline will be deposited is 0.1076μg. In case of polyaniline deposited on bare ITO, the whole ITO surface is exposed to the solution and it will be around 1.14 μg.

We also examined the electrochemical capacitance performance of both the material (PANI nanorods and PANI deposited on bare ITO using identical condition) by charge discharge cycle. The specific capacitance values were calculated by charge discharge cycling measurement which is considered to be the most reliable. Specific capacitance[S1] is given by (Fg^{-1}) $=i(A) \times \Delta t(s)/\ \Delta E(V) \times m(g)$. Here, i is the discharge current in amperes, Δt is the discharge time in second corresponding to the voltage difference ΔE in volts and m is the electrode mass in grams.

S7. Calculation of capacitance of polyaniline deposited on bare ITO

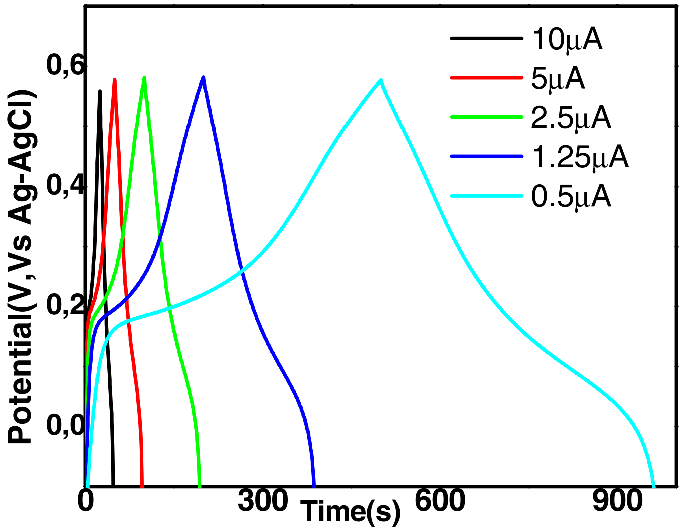

Figure S8 Charge discharge test of polyaniline thin film deposited on blank ITO at different current in 0.5M H_2SO_4.

From the charge discharge cycle, we have calculated the specific capacitance of PANI on ITO and it is around 299 Fg^{-1} at current 0.5 µA. The specific capacitance value of polyaniline deposited on bare ITO is also supported by the reported value in the literature[S6,S7].

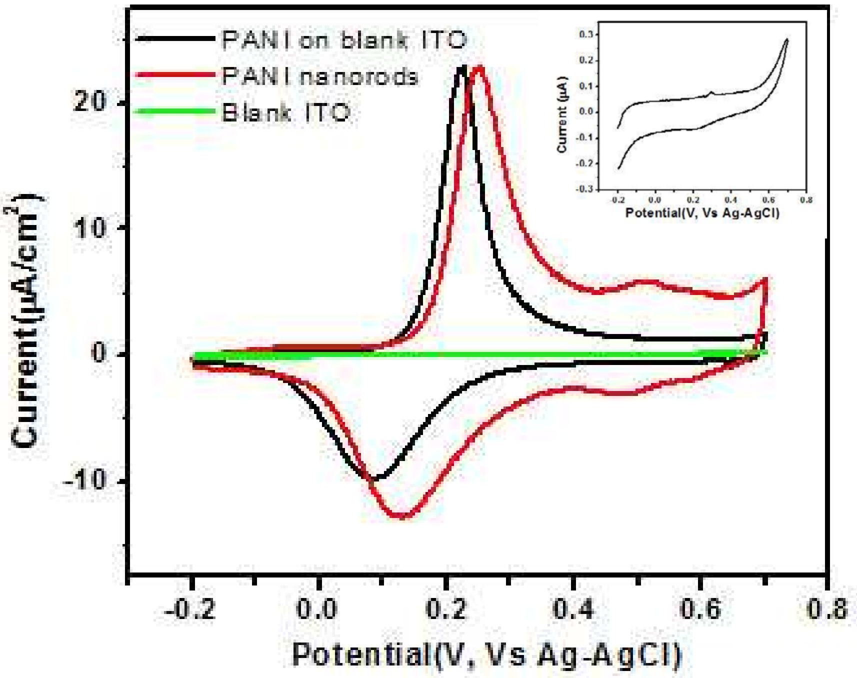

Figure S9. CV study of polyaniline nanorods and polyaniline thin film on bare ITO at scan rate of 20mv/S. [Inset shows CV of bare ITO at same scan rate]

We have also tried to perform the charge/discharge experiment of bare ITO with the same electrolyte but it did not show any characteristic charge/discharge curve in the current densities we used for other samples. If we compare the CV curves (Figure S9*)*, it is seen that the CV curve of bare ITO is close to rectangular shape produced by double layer capacitance characteristics of the electrode and is distinct from the CV curve of PANI nanorods and PANI deposited on bare ITO. In this case, the Faradic current (inset of Figure.S9) relating to double layer capacitance is very small (0.06μA at 0.249V) compared to PANI material. Hence, the contribution for the capacitance from bare ITO is very small and can be neglected. It is also reported in the literature[S7,S8] that the specific capacitance for doped tin oxide is around 8µF\cm^{-2} which is quite insignificant compared to that reported for the PANI nanorods.

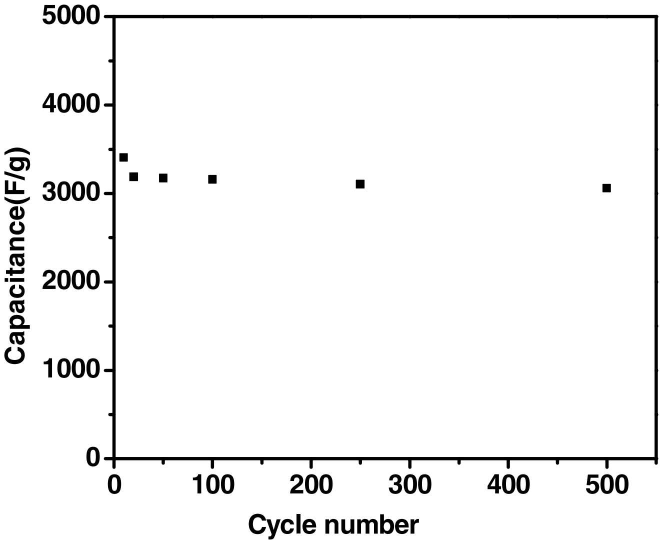

Figure S10. Charge discharge cycle of polyaniline nanorods at current 10 µA within the potential window 0.69V to -0.1 V vs Ag-AgCl

We have also performed the experiments for electrochemical stability (Figure. S10) of the polyaniline nanorods upto 1000 cycle. However, we observed that up to 500 cycles they show good charge/discharge cycle but after that these polyaniline nanorods do not show regular charge/discharge cycle and behave abnormally. This may be due to the lower stability of the very small dimension polyaniline nanorods. As these small nanorods are not chemically grafted to the ITO surface, they may go to the solution from the ITO substrate for longer charge/discharge cycles.

S8. UV-vis study of the polyaniline nanorods:

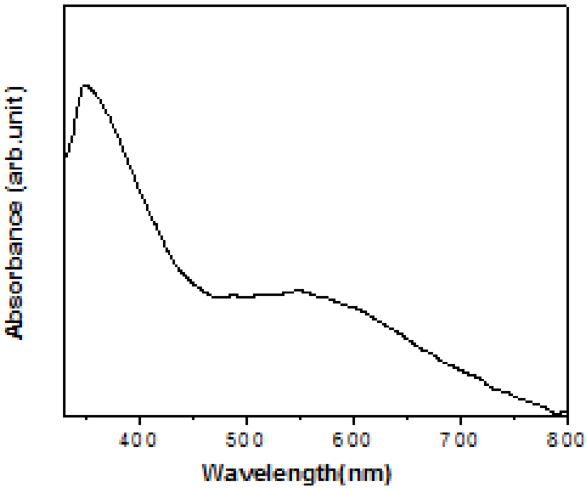

Figure S11. UV-vis spectra of polyaniline nanorods

Figure S11 shows two absorption peak for PANI nanorods. The peak at 345 nm is because of π-π^* transition and a broad peak from 500 to 800 nm centered around at 600 nm is due to the excitation formation of quinoid ring corresponding to the semi-conducting phase of PANI-$HClO_4$ nanorods.

References:

S1. Y.-G. Wang, H.-Q. Li, Y.-Y. Xia, *Adv. Mater.*, 2006, **18**, 2619.

S2. W. Zheng, M. Angelopoulos, A. J. Epstein, A. G. MacDiarmid, *Macromolecules*, 1997, **30,** 2953.

S3. Y. Wei, K. F. Hsueh, G. W. Jang, *Macromolecules*, 1994, **27**, 518.

S4. S. Licoccia, M. Trombetta, D. Capitani, N. Proietti, P. Romagnoli, M. L. D. Vona, *Polymer,* 2005, **46**, 4670.

S5. Y.-Y. Horng, Y.-K. Hsu, A. Ganguly, C.-C. Chen, L.-C. Chen, K. H. Chen, *Electrochem. Commun.*, 2009, **11**, 850.

S6. C. A. Amarathan, J. H. Chang, D. Kim, R. S. Mane, S.-H. Han, D. Sohn, *Mater. Chem. Phys.*, 2009, **113,** 14.

S7. F. Montilla, M.A. Cotarelo, E. Morallon, *J. Mater. Chem.,* 2009, **19**,305.

S8. F. Montilla, E. Morallón, A. De Battisti, J. L. Vázquez, *J. Phys. Chem., B,* 2004, **108,** 5036.